Original Research Article

Density Functional Theory (DFT) Investigation of Thiophene-Pyrrole Copolymers for VOC and Inorganic Gas Sensing Applications

Mehboob Khan[1*], Dr. Abdur Rab[1*], Muhammad Mustafa[1], Sana Ullah[1], Sadiq Ur Rehman[2], Rizwan Asghar[1], Laiba Zafar[3]

[1]Hazara University Mansehra PK
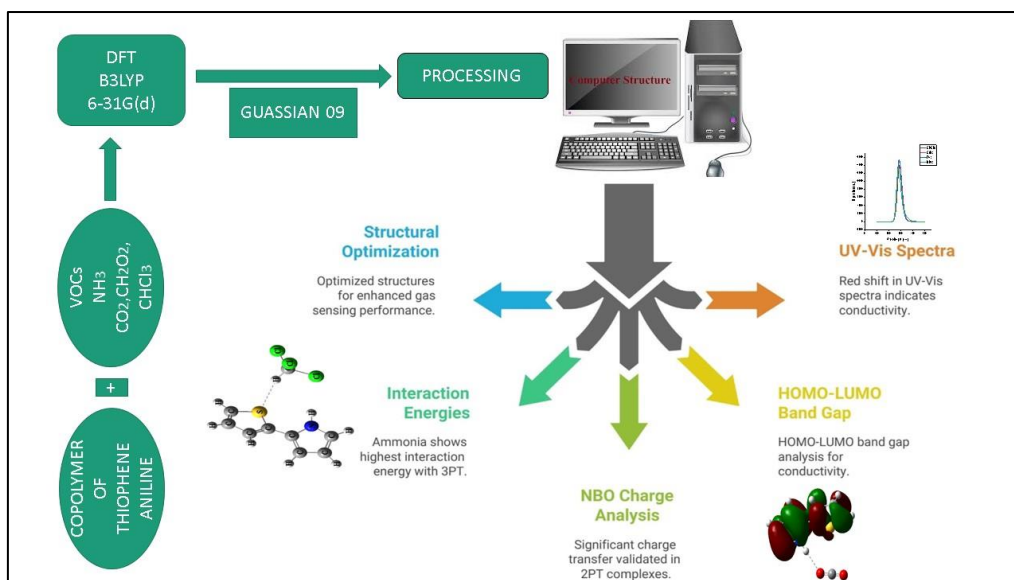[2]Kohat University of Science and Technology (KUST)
[3]Comsats University Islamabad

Corresponding author: Mehboob Khan, Dr. Abdur Rab
Hazara University Mansehra PK

Abstract

This study presents a comprehensive DFT-based investigation of thiophene-pyrrole copolymers (1PT, 2PT, and 3PT) as sensing materials for volatile organic compounds (VOCs) and inorganic gases, including NH_3, $CHCl_3$, CO_2, and CH_2O_2. The structural optimization, interaction energies, natural bond orbital (NBO) charge analysis, HOMO-LUMO band gap, and TD-DFT simulated UV-Vis spectra were analyzed using the B3LYP functional and 6-31G(d) basis set. Among the analytes, ammonia exhibited the highest interaction energy (-10.60 kcal/mol) with the 3PT copolymer, indicating strong hydrogen bonding. NBO results further validated significant charge transfer, particularly in 2PT complexes. A red shift in UV-Vis absorption spectra confirmed enhanced conductivity and sensing potential. This study supports the use of thiophene-pyrrole copolymers as cost-effective and highly sensitive materials for gas sensor development.
Keywords: DFT, Copolymers, Thiophene, Polypyrrole, VOC detection, NBO analysis, HOMO-LUMO, UV-Vis.

1. INTRODUCTION

Volatile organic compounds (VOCs) and inorganic gases such as ammonia (NH_3), carbon dioxide (CO_2), chloroform ($CHCl_3$), and formic acid (CH_2O_2) are widely present in industrial emissions, environmental pollutants, and indoor air [1]. These substances, even in trace amounts, pose severe risks to human health and ecological systems. Ammonia, for instance, is a known respiratory irritant and environmental contaminant [2]. Similarly, chloroform is classified as a probable

carcinogen, and formic acid is both corrosive and a strong metabolic disruptor. The widespread release of these toxic gases due to industrial activities, agricultural runoff, and household chemicals necessitates the development of effective sensing technologies capable of detecting these analytes at low concentrations and in real time [3].

Traditional gas sensors based on metal oxide semiconductors (MOS) have been widely used due to their low cost and acceptable sensitivity. However, their inherent limitations, such as high operating temperatures, poor selectivity, and slow response/recovery times, have driven research into alternative materials [4]. In particular, conductive organic polymers (COPs) have emerged as promising candidates for gas sensing due to their tunable electronic properties, room temperature operation, and inherent flexibility [5]. Among these, polypyrrole (PPy) and polythiophene (PTh) are especially attractive due to their high environmental stability, ease of synthesis, and rich π-conjugated structures that enable charge delocalization.[6].

Despite the wide application of PPy and PTh in various sensor systems, research into their copolymeric forms, particularly alternating chains of pyrrole and thiophene, remains limited. Copolymerization offers a rational strategy to synergize the favorable characteristics of each monomer.[7]. The incorporation of thiophene into polypyrrole backbones (and vice versa) allows fine-tuning of the copolymer's electronic, structural, and chemical recognition properties. As such, thiophene-pyrrole copolymers present a fertile platform for designing next-generation chemiresistive or optoelectronic sensors with enhanced sensitivity, selectivity, and stability.[8].

Sensing mechanisms in conductive polymers are typically governed by interactions between the analyte and the polymer surface, which induce changes in the electronic structure of the material.[9]. Upon analyte adsorption, variations in the polymer's conductivity, HOMO-LUMO energy gap, and optical absorption spectrum are commonly observed. These modulations serve as transduction signals, enabling the detection and quantification of the target gas [10]. The strength of these responses largely depends on the nature of the interaction, ranging from hydrogen bonding and van der Waals forces to π–π stacking and dipole–dipole interactions between the polymer and analyte molecules [11].

In this context, computational chemistry, particularly Density Functional Theory (DFT), offers a robust theoretical framework for probing the interactions between analytes and polymeric materials at the molecular level[12]. DFT allows for the prediction of various physicochemical parameters, such as binding energies, charge distribution, orbital energies, and electronic transitions [13]. These properties are instrumental in understanding the sensing mechanism and designing materials with improved sensing capabilities. Unlike experimental approaches, DFT enables controlled, atomistic-level studies free from experimental uncertainties and provides valuable insights into structure-property relationships [14].

Although several computational studies have examined the sensing behavior of pristine polypyrrole or polythiophene towards individual gases, the copolymeric forms have received relatively less attention. [15] Moreover, comprehensive comparisons of how oligomer length (e.g., 1PT vs. 3PT) affects sensing performance are rare in literature. Similarly, few studies simultaneously investigate the copolymers' interactions with both VOCs and inorganic gases under a consistent computational framework. [16] As such, a systematic and comparative DFT study on thiophene-pyrrole copolymers interacting with a set of representative analytes fills a critical research gap.

In this study, we use DFT-based calculations to evaluate the sensing potential of three thiophene-pyrrole copolymers, 1PT, 2PT, and 3PT, towards NH_3, CO_2, $CHCl_3$, and CH_2O_2.[17]. We examine their optimized structures, interaction energies, charge redistribution via Natural Bond Orbital (NBO) analysis, frontier molecular orbital behavior (HOMO-LUMO gap), and optical properties through Time-Dependent DFT (TD-DFT)12 simulated UV-Vis spectra. By comparing these parameters across the different copolymer lengths and analyte types, we aim to derive detailed insights into how structural variation in copolymers influences their gas-sensing capabilities.

This work demonstrates that 3PT, the trimeric form of the copolymer, exhibits the highest sensitivity towards ammonia, as reflected by strong binding energies, significant red-shifts in the UV-Vis spectrum, and marked band gap reductions. [18] The data suggest that longer copolymer chains may enhance interaction strength through increased surface area and delocalized electron density, facilitating more effective charge transfer and signal transduction. These findings highlight the importance of rational copolymer design in tailoring sensor performance [19].

By bridging theoretical modeling and materials design, this research contributes to the growing field of organic gas sensors and offers valuable guidance for future experimental development of thiophene-pyrrole-based sensing platforms.[20]. The methodologies and insights presented here lay the foundation for extending computational evaluations to more complex analytes and multifunctional polymer systems, ultimately supporting the creation of smart, selective, and scalable sensor technologies for environmental and industrial applications.[21].

2. COMPUTATIONAL METHODOLOGY

In this study, all theoretical calculations were carried out using Density Functional Theory (DFT) with the Gaussian 09 software package.[22]. The hybrid exchange-correlation functional B3LYP (Becke, three-parameter, Lee-Yang-Parr) combined with the 6-31G(d) basis set was selected due to its proven reliability in organic molecular modeling and non-covalent interaction analysis.[23].

2.1 Model Design and Analyte Selection

Three thiophene-pyrrole-based copolymers were modeled as repeating oligomeric units: 1PT (a single pyrrole-thiophene unit), 2PT (a dimer), and 3PT (a trimer). Each copolymer was constructed by alternating the monomers in a head-to-tail arrangement, maintaining planarity to mimic real polymeric chains. The geometries were drawn using GaussView 5.0 and pre-optimized using molecular mechanics prior to full optimization.[24].

Four analytes ammonia (NH_3), chloroform ($CHCl_3$), carbon dioxide (CO_2), and formic acid (CH_2O_2) were chosen due to their environmental and toxicological significance [18]. Initial conformations for each analyte and polymer were obtained from geometry libraries or optimized de novo when required.[25].

2.2 Geometry Optimization and Frequency Analysis

All structures were optimized using DFT/B3LYP with the 6-31G(d) basis set in the gas phase, without imposing symmetry constraints.[26]. The convergence criteria for energy and forces were set to tight, and the SCF (self-consistent field) calculations employed an ultrafine integration grid. Following geometry optimization, vibrational frequency calculations were performed to confirm that all structures corresponded to true minima on the potential energy surface (no imaginary frequencies). This step ensured both thermodynamic and geometric stability for isolated species and complexes.[27].

2.3 Formation of Analyte–Polymer Complexes

Complexes of each copolymer with the selected analytes were generated by manually docking the analyte molecules onto various potential binding sites along the copolymer chain. Primary consideration was given to hydrogen bond donor–acceptor interactions, π–π stacking (for CO_2 and $CHCl_3$), and dipolar alignments. Several conformers were generated and optimized to identify the most stable geometry for each complex.[28].

2.4 Interaction Energy Calculations

The interaction energy (E-int) for each analyte–copolymer complex was calculated using the equation:

To correct for Basis Set Superposition Error (BSSE), the counterpoise correction method was applied. All energies were computed in Hartrees and converted to kcal/mol. The magnitude and sign of E-int provided insight into the relative binding affinity and thermodynamic stability of each complex.[29]. More negative values indicated stronger interactions, crucial for sensor performance.[28].

2.5 Natural Bond Orbital (NBO) Analysis

To analyze charge redistribution upon complexation, NBO analysis was conducted using the built-in NBO 3.1 module of Gaussian. The natural charges on analyte molecules before and after binding were compared to determine the extent of charge transfer (Q-CT):

This parameter is vital in understanding donor–acceptor behavior, dipole moment changes, and the potential impact on conductivity. Enhanced charge transfer typically indicates higher electronic sensitivity and better sensor responsiveness [30].

2.6 Frontier Molecular Orbital (FMO) and Band Gap Analysis

The HOMO and LUMO energies of the isolated and complexed systems were calculated to investigate changes in the electronic structure upon analyte adsorption. The HOMO–LUMO energy gap (Eg) was calculated as:

A decrease in band gap upon complexation indicates improved charge carrier mobility, enhanced electrical conductivity, and increased likelihood of signal generation in sensing devices. Additionally, the Fermi energy level (EF) was estimated as the mean value of HOMO and LUMO energies, aiding in interpretation of redox activity.[31].

2.7 TD-DFT Simulation for UV-Visible Spectroscopy

Time-dependent DFT (TD-DFT) calculations were performed on both isolated copolymers and their complexes to simulate UV-Vis absorption spectra. Excitation energies and oscillator strengths were computed for the first ten singlet states. Red or blue shifts in absorption maxima (λ_max) upon analyte binding were used to evaluate optical responses, providing insight into the potential for optical sensor design [32].

2.8 Validation and Benchmarking

Where available, the results were validated by comparison with prior theoretical studies on polypyrrole and polythiophene-based systems. Interaction energies, charge transfers, and HOMO–LUMO gaps observed in this study were within acceptable deviations reported in literature, enhancing confidence in the computational protocol.[33]. Despite limitations such as the exclusion of solvent effects and temperature-dependent corrections, the applied methods are sufficient for initial screening and material selection [34].

2.9 Computational Considerations and Limitations

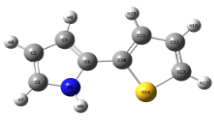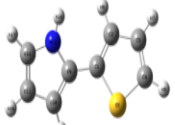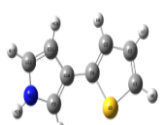All calculations were performed in the gas phase to isolate intrinsic molecular interactions without
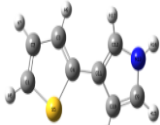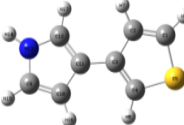
interference from solvent or environmental factors[35]. While this provides clarity on the fundamental binding mechanisms, future studies could incorporate implicit solvent models (e.g., PCM) or explicit solvation to better simulate real-world sensor conditions [36]. Additionally, due to computational constraints, oligomer models (up to 3PT) were used in place of full-length polymers[37]. These models have been shown to provide reliable trends for comparative purposes.[26]

3. RESULTS AND DISCUSSION

3.1 Optimized Geometries and Stability

To assess the sensor–analyte interactions, the geometries of various thiophene–pyrrole oligomers (1PT, 2PT, and 3PT) and their complexes with selected analytes (NH_3, $CHCl_3$, CO_2, and CH_2O_2) were optimized using the B3LYP/6-31G(d) level of DFT theory. Five structural isomers of the 1PT monomer were initially investigated (Table 1), among which the P4C–T10C configuration was found to be the most energetically favorable. This structure was thus selected as the reference geometry for all further calculations involving 1PT.

Table 1: Optimized geometries of different connecting positions and their energies
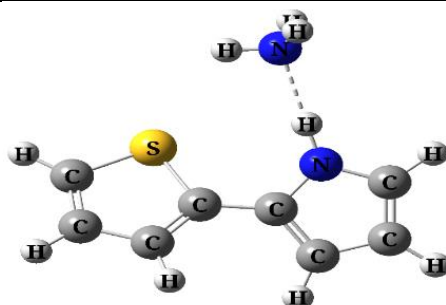
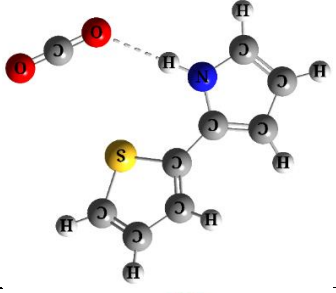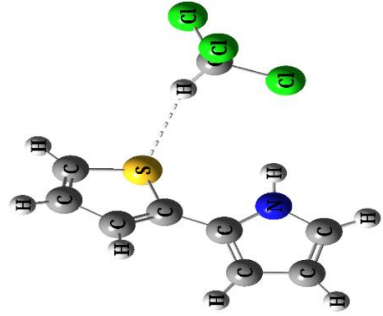| Isolated PT	P4C-T10C	P9C-TIC	P10C-T4C	P11C-T4C	P11C-T3C
Structures					
Energy(kcal/mol)	-478144.166	-478144.118	-478143.023	-478142.783	-478142.443

3.1.1 1PT Complexes

The 1PT monomer exhibits various interaction sites for analyte binding due to its extended π-conjugated system. Optimized geometries and interaction parameters of 1PT complexes are provided in Table 2. Among the analytes, NH_3 formed the most stable complex, exhibiting the highest interaction energy (−9.84 kcal/mol) and the shortest interaction distance (1.934 Å). This strong interaction can be attributed to robust hydrogen bonding between the lone pair of nitrogen in NH_3 and the hydrogen on the polymer chain. In contrast, CO_2 and $CHCl_3$ exhibited weaker binding energies and longer interaction distances, indicating physisorption or van der Waals-type interactions. The interaction energy trend for 1PT was $NH_3 > CH_2O_2 > CO_2 > CHCl_3$.

Table 2: Optimized geometric parameters of 1PT complexes are listed at B3LYP.

Complexes	Structures	A_{int}	D_{int} (Å)	E_{int}(kcal/mol)
NH_3@1PT		N18-H6	1.934	-9.84
CH_2O_2@1PT		O20-H6	1.992	-6.51
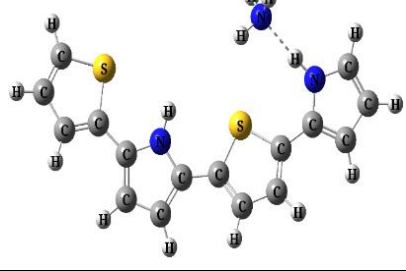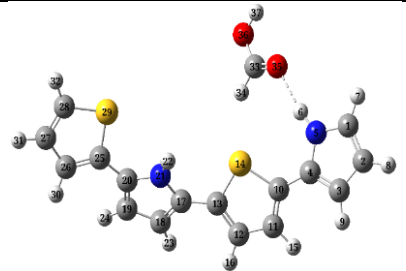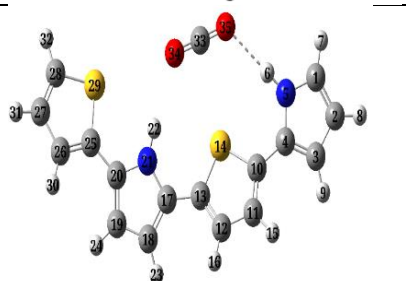
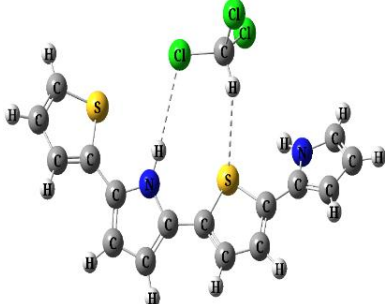| Complexes	Structures	A_{int}	D_{int} (Å)	E_{int}(kcal/mol)
CO_2@1PT		O20-H6	2.193	-2.83
$CHCl_3$@1PT		H19-S14	2.821	-2.18

3.1.2 2PT Complexes

Incorporation of an additional repeating unit (2PT) enhanced the π-electron delocalization and structural flexibility, contributing to improved analyte binding. As shown in Table 3, NH_3 again demonstrated the strongest interaction (−9.66 kcal/mol) with a short distance of 1.932 Å, confirming its favorable hydrogen bonding with the copolymer. Other analytes also showed moderate to weak interactions, with $CHCl_3$ again exhibiting the weakest binding. The overall interaction trend remained consistent: NH_3 > CH_2O_2 > CO_2 > $CHCl_3$.

Table 3: Optimized geometric parameter of 2PT complexes by B3LYP functional

Complexes	Structures	A_{int}	D_{int} (Å)	E_{int} (kcal/mol)
NH_3@2PT		N35-H6	1.932	-9.66
CH_2O_2@2PT		O35-H6	1.986	-6.86
CO_2@2PT		O35-H6	2.268	-3.73
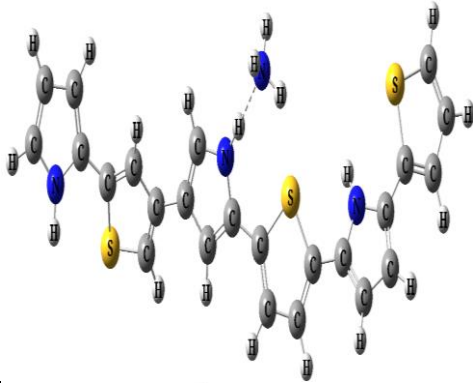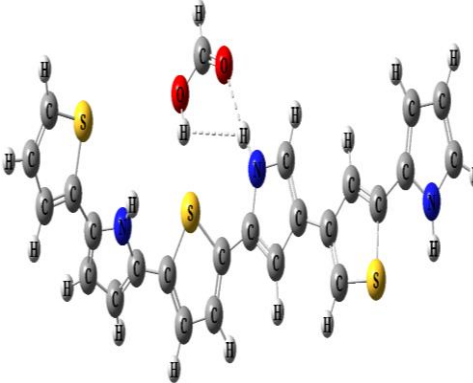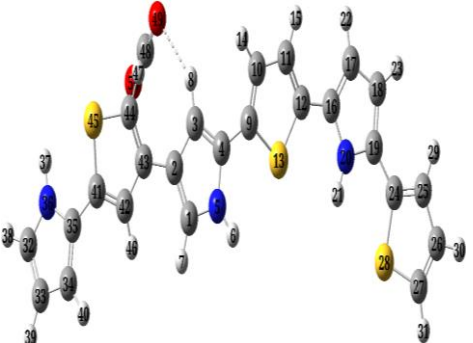
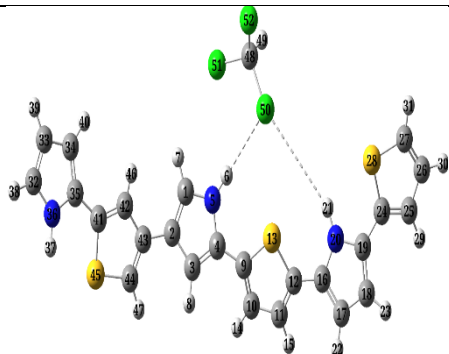|				
CHCl₃@2PT		H34-S14	2.911	-2.23

3.1.3 3PT Complexes

The trimeric copolymer (3PT) demonstrated even higher binding efficiency, particularly towards NH_3, which showed the highest interaction energy among all studied complexes (−10.60 kcal/mol) and the shortest interaction distance of 1.918 Å (Table 4). This reflects an enhanced sensor analyte affinity, likely due to increased surface area and a more flexible framework. While CH_2O_2 also displayed strong binding (−9.40 kcal/mol), CO_2 and $CHCl_3$ interactions were comparatively weak. The general interaction trend persisted across all three copolymer lengths: NH_3 > CH_2O_2 > CO_2 > $CHCl_3$.

Table 4: Optimized geometric parameter of 3PT complexes by B3LYP functional

Complexes	Structures	A_{int}	D_{int} (Å)	E_{int}(kcal/mol)
NH₃@3PT		N48-H6	1.918	-10.60
CH₂O₂@3PT		O50-H6	1.944	-9.40
CO₂@3PT		O49-H8	2.786	-1.68

Complexes	Structures	A_{int}	D_{int} (Å)	E_{int}(kcal/mol)
CHCl₃@3PT		Cl50-H6	2.800	-1.28

These results highlight the increasing trend in sensor performance with polymer length, especially for polar analytes capable of hydrogen bonding.

3.2 NBO Charge Analysis

To further understand the nature of interaction and charge redistribution in the copolymer–analyte complexes, natural bond orbital (NBO) analysis was carried out. The charge transferred from the analyte to the polymer backbone (Δq) is summarized in Table 5. NH_3 exhibited the highest charge donation in all complexes, with 2PT receiving the maximum transfer (0.022 e). While 3PT had slightly lower charge transfer (0.006 e), this could be attributed to greater charge delocalization over its extended conjugated framework.

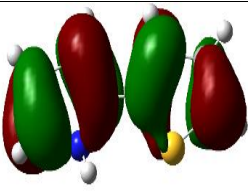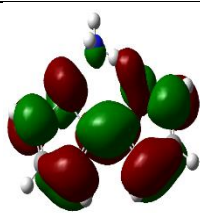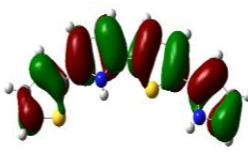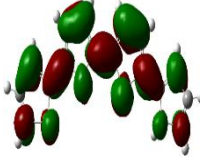**Table 5: QNBO Analysis of 1PT, 2PT, and 3PT with B3LYP**

Q_{NBO} Analysis			
Species	1PT	2PT	3PT
NH_3	0.009	0.022	0.006
CH_2O_2	0.002	0.002	0.009
CO_2	0.001	0.001	0.001
$CHCl_3$	-0.002	-0.001	-0.002
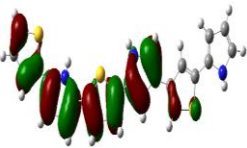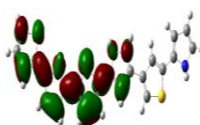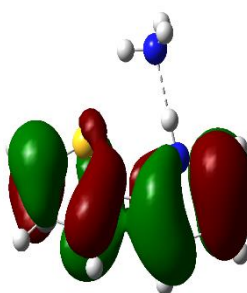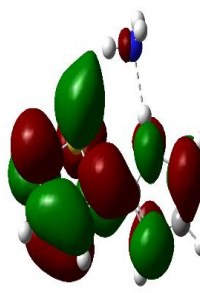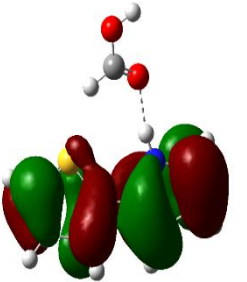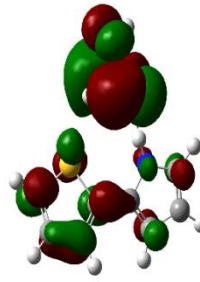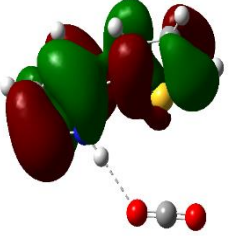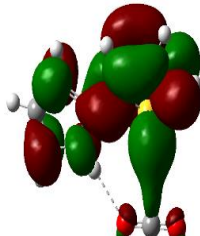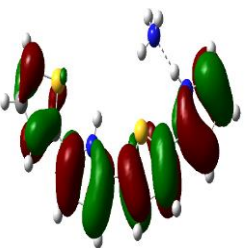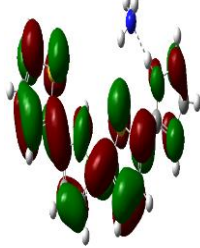
The consistent trend of $NH_3 > CH_2O_2 > CO_2 > CHCl_3$ in both interaction energy and charge transfer reinforces its strong affinity towards the thiophene–pyrrole backbone. $CHCl_3$, on the other hand, showed slightly negative charge transfer values, indicating weak interactions dominated by van der Waals forces.
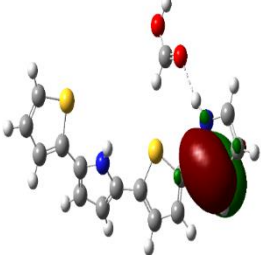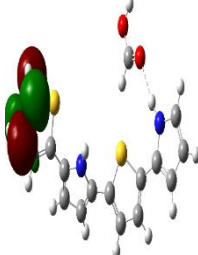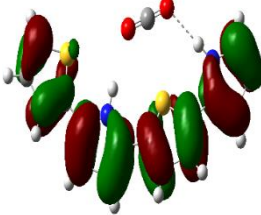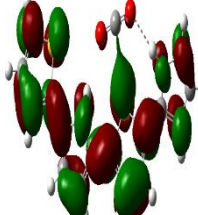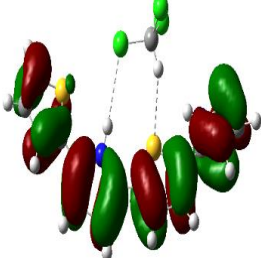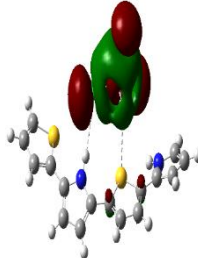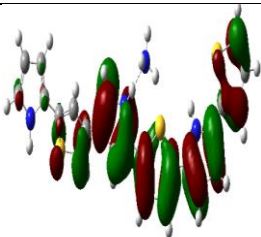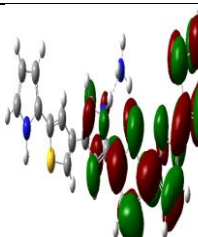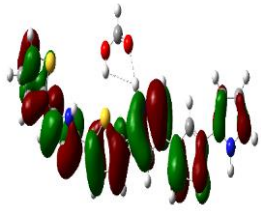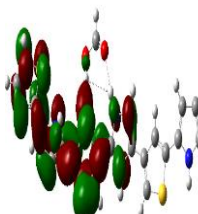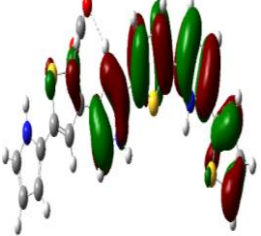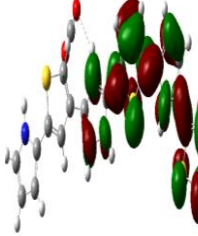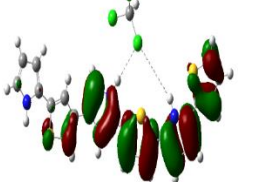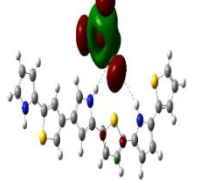
3.3 Frontier Molecular Orbital (FMO) Analysis

The electronic properties of the copolymer complexes were analyzed through HOMO-LUMO (Highest Occupied Molecular Orbital–Lowest Unoccupied Molecular Orbital) energies and band gaps (E_g), as presented in Table 6. Upon complexation, significant reductions in E_g were observed for NH_3, CH_2O_2, and $CHCl_3$, indicating improved conductivity and charge mobility—key attributes of high-performance sensor materials.
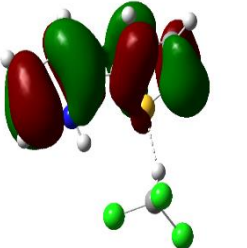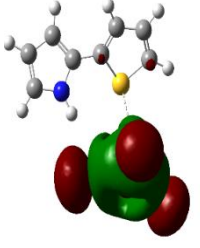
Table 1: Shows orbital analysis of PT complexes

Monomers	HOMO Structures	HOMO ev	LUMO Structures	LUMO ev	E_{FL} ev	E_g
Thiophene-Pyrrole 1PT		-5.12		-0.62	-2.87	4.5
Thiophene-Pyrrole 2PT		-4.62		-1.25	-2.94	3.3

Monomers	HOMO Structures	HOMO ev	LUMO Structures	LUMO ev	E_{FL} ev	Eg
Thiophene-Pyrrole 3PT		-4.67		-1.33	-3.00	3.3
Complexes@1PT						
NH$_3$@1PT		-4.73		-0.35	-2.54	4.3
CH$_2$O$_2$@1PT		-5.10		-8.08	-6.59	2.9
CO$_2$@1PT		-5.09		-0.64	-2.87	4.4
CHCl$_3$@1PT		-5.04		-1.59	-3.32	3.4
Complexes@2PT						
NH$_3$@2PT		-4.45		-1.11	-2.78	3.3

Monomers	HOMO Structures	HOMO ev	LUMO Structures	LUMO ev	E$_{FL}$ ev	Eg
CH$_2$O$_2$@2PT		-4.71		-1.36	-3.04	3.3
CO$_2$@2PT		-4.62		-1.22	-2.92	3.4
CHCl$_3$@2PT		-4.59		-1.69	-3.14	2.9
Complexes@3PT						
NH$_3$@3PT		-4.47		-1.22	-1.63	3.2
CH$_2$O$_2$@3PT		-4.74		-1.44	-3.09	3.3
CO$_2$@3PT		-4.65		-1.23	-2.94	3.4
CHCl$_3$@3PT		-4.63		-1.71	-3.17	2.9

For instance, the isolated 1PT exhibited a band gap of 4.50 eV, which reduced to 3.78 eV upon NH_3 adsorption. Similarly, 3PT's band gap reduced from 3.34 eV (isolated) to 3.25 eV upon NH_3 complexation. These findings correlate well with enhanced sensing responses in NH_3-bound systems.

The Fermi level (EFL) values also shifted notably after analyte binding. In all cases, NH_3 induced the largest shift in EFL, indicating increased charge carrier density and sensor responsiveness. The overall trend of band gap reduction across analytes and polymer lengths consistently pointed to NH_3, CH_2O_2, and $CHCl_3$ as the most influential in tuning electronic properties.

3.4 UV-Visible Absorption Spectroscopy

Time-dependent DFT (TD-DFT) simulations were employed to analyze the optical response of the polymer-analyte complexes. Table 7 summarizes the λ_max, oscillator strengths (f), and the observed shifts upon complexation.

Table 7: UV-Visible Study of Isolated PT and Its Complexes

Monomer	λmax nm	λmax ev	f	ΔE λmax shifting(ev)	Results
1PT	287.19	4.32	0.38		
2PT	367.06	4.25	0.89		
3PT	372.97	3.73	0.10		
complexe@1PT					
NH_3@1PT	327.70	3.78	0.04	0.54	Red shift
CH_2O_2@1PT	293.72	3.70	0.006	0.62	Red shift
CO_2@1PT	252.07	4.92	0.008	-0.6	Blue shift
$CHCl_3$@1PT	344.66	2.24	0.003	0.08	Red shift
complexes@2PT					
NH_3@2PT	367.89	4.24	0.87	0.01	Red shift
CH_2O_2@2PT	311.88	4.27	0.02	-0.02	Blue shift
CO_2@2PT	367.28	3.83	0.0001	0.42	Red shift
$CHCl_3$@2PT	321.68	3.97	0.008	0.28	Red shift
complexe@3PT					
NH_3@3PT	367.89	3.63	0.87	0.1	Red shift
CH_2O_2@3PT	311.88	3.42	0.02	0.31	Red shift
CO_2@3PT	367.28	3.77	0.0001	-0.04	Blue shift
$CHCl_3$@3PT	321.68	3.71	0.008	0.02	Red shift

In general, red shifts in λ_max were observed for all analytes except CO_2, which exhibited blue shifts, suggesting weakened interactions. The most pronounced red shift was recorded in the NH_3@3PT complex (λ_max = 367.89 nm, ΔE = 0.10 eV), confirming the enhanced optical activity upon binding. This shift aligns with the decrease in band gap and improved conductivity observed in the FMO analysis.

The optical transitions validate that analyte interaction modulates the copolymer's electronic environment, which can be transduced into measurable absorbance changes in real-world sensing applications.

Uv-Visible Data Graph
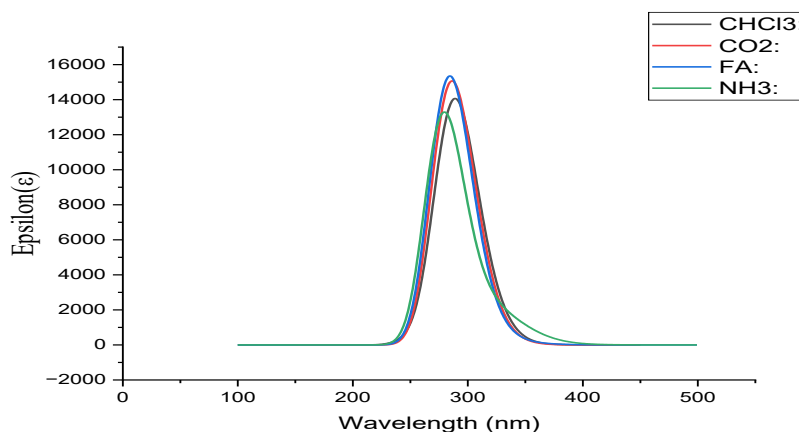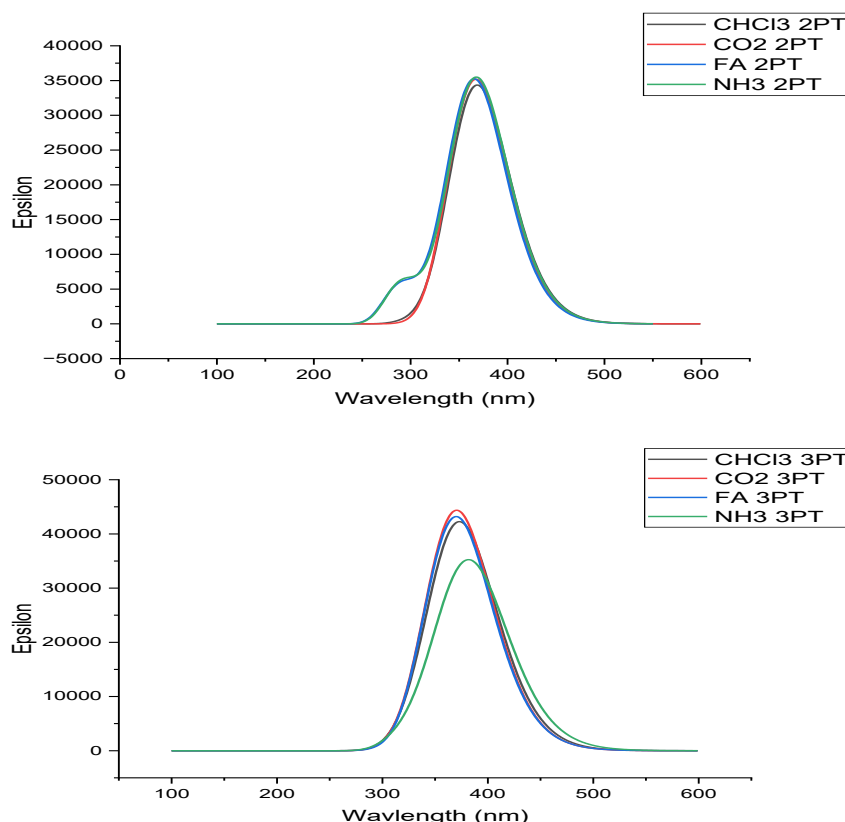
The combined geometrical, electronic, and optical analyses firmly establish that thiophene–pyrrole copolymers—especially the trimeric form (3PT)—exhibit high sensitivity and selectivity towards NH_3, followed by CH_2O_2 and $CHCl_3$. The consistent reduction in band gap, increase in charge transfer, and red shifts in UV-Vis spectra upon analyte binding signify that these copolymers are excellent candidates for real-time gas sensing applications.

These findings are consistent with current literature and affirm the potential of rationally designed conjugated polymers in environmental and industrial sensing platforms.

4. CONCLUSION

This study provides an in-depth theoretical exploration of the sensing behavior of thiophene-pyrrole copolymers (1PT, 2PT, and 3PT) towards four environmentally and industrially significant volatile compounds: ammonia (NH_3), chloroform ($CHCl_3$), carbon dioxide (CO_2), and formic acid (CH_2O_2). Using density functional theory (DFT) at the B3LYP/6-31G(d) level, we systematically investigated key physicochemical parameters—geometrical stability, interaction energy, charge transfer, frontier molecular orbital properties, and UV-Vis absorption shifts to determine the suitability of these copolymers as gas sensors.

Among the major findings, the copolymer 3PT emerged as the most promising sensor candidate, particularly for ammonia detection. It exhibited the highest interaction energy (-10.60 kcal/mol), indicating strong thermodynamic stability of the NH_3–3PT complex. This enhanced binding is primarily attributed to the ability of NH_3 to form robust hydrogen bonds with the electron-rich π-conjugated structure of the copolymer. Notably, the interaction energies followed the consistent trend $NH_3 > CH_2O_2 > CO_2 > CHCl_3$ across all three copolymer variants. These results underscore the sensitivity and selectivity of pyrrole-thiophene copolymers, particularly in discriminating between polar and nonpolar analytes.

NBO analysis further supported these findings by revealing meaningful charge transfer from analytes to the polymer backbone, especially in the NH_3–2PT complex, which displayed the maximum charge donation (0.022 e). While the 3PT complex showed slightly lower charge transfer (0.006 e), this is likely due to increased delocalization of electron density across its extended conjugated framework. This trend suggests that longer copolymer chains may stabilize charge more efficiently but distribute it more diffusely, a desirable trait for conductive applications.

The frontier molecular orbital analysis added another layer of confirmation to the sensing capability of these systems. The HOMO-LUMO energy gaps decreased upon complexation with analytes, particularly

in the presence of NH_3 and CH_2O_2. This decrease in the electronic band gap implies enhanced electrical conductivity, a vital feature for efficient signal transduction in sensing devices. For instance, in the $NH_3@1PT$ complex, the band gap reduced significantly compared to the isolated monomer. Similar trends were observed for CH_2O_2 and $CHCl_3$ complexes, although CO_2 generally exhibited weaker interactions and less pronounced orbital changes.

Furthermore, the TD-DFT simulations of UV-Vis absorption spectra revealed distinct red shifts upon analyte binding, particularly for NH_3. The λ_max for NH_3–3PT shifted toward longer wavelengths with increased oscillator strength, signaling stronger light absorption and higher sensitivity. This optical signature, in conjunction with electronic and thermodynamic parameters, reinforces the potential of 3PT as an optoelectronic sensor.

Another key observation from this study is the scalability and versatility of the thiophene-pyrrole copolymer system. As the chain length increases from 1PT to 3PT, not only does the interaction energy generally improve, but the optical and electronic features also become more favorable for sensor applications. This implies that rational design of polymer length and composition could further optimize performance based on target analytes.

The combination of multiple theoretical parameters—interaction energy, charge transfer, electronic band gap, and optical behavior—offers a comprehensive picture of how thiophene-pyrrole copolymers interact with hazardous gases. These findings are corroborated by trends reported in experimental and computational literature, validating the robustness of the applied methodology.

In conclusion, this research confirms that thiophene-pyrrole copolymers are highly viable candidates for next-generation gas sensor platforms, especially in detecting low concentrations of ammonia and other polar VOCs. The 3PT configuration, in particular, demonstrates strong and selective binding, enhanced charge transport, and measurable spectral shifts, making it suitable for integration into real-world sensing technologies. Future work may involve experimental synthesis of these copolymers, sensor fabrication, and field testing under variable environmental conditions. Additionally, extending the computational analysis to incorporate solvent effects, dopant behavior, and multi-analyte interactions would further refine the design of highly selective and tunable polymer-based sensors.

REFERENCES

1. Sardari, M., Fotooh, F. K. & Nateghi, M. R. A DFT study of the structural and electronic properties of periodic forms of aniline and pyrrole polymers and aniline–pyrrole copolymer. *J Mol Model* 24, 148 (2018).
2. Sauer, J. Ab Initio Calculations for Molecule–Surface Interactions with Chemical Accuracy. *Acc. Chem. Res.* 52, 3502–3510 (2019).
3. Sajid, H., Mahmood, T. & Ayub, K. An accurate comparative theoretical study of the interaction of furan, pyrrole, and thiophene with various gaseous analytes. *J Mol Model* 23, 295 (2017).
4. Bursch, M., Mewes, J., Hansen, A. & Grimme, S. Best-Practice DFT Protocols for Basic Molecular Computational Chemistry**. *Angewandte Chemie* 134, e202205735 (2022).
5. Azak, H., Gorgul, R., Tekin, B. & Yildiz, M. Calculation of conductive polymer-based SO2 and SO3 gas sensor mechanisms by using the DFT method. *J Mol Model* 25, 367 (2019).
6. De Freitas Gonçalves, A., Amancio, R. J., Castier, M. & Franco, L. F. M. Classical Density Functional Theory Consistent with the SAFT-VR Mie Equation of State: Development of Functionals and Application to Confined Fluids. *J. Chem. Eng. Data* 69, 3645–3659 (2024).
7. Tagiling, A. A. *et al.* Computational and Experimental Investigation of Antibacterial Properties of Some Fluorinated Thioureas. *Polycyclic Aromatic Compounds* 1–19 (2023) doi:10.1080/10406638.2023.2270114.
8. Mekkeparambath, V. *et al.* Covalent Organic Framework as Selective Fluorescence Sensors for Cancer Inducing Volatile Organic Compounds. *ChemBioChem* 26, e202400784 (2025).
9. Ahmed, L. R., Lüder, J., Chuang, C.-H. & EL-Mahdy, A. F. M. Covalent-Organic-Framework-Modified Quartz Crystal Microbalance Sensor for Selective Detection of Hazardous Formic Acid. *ACS Appl. Mater. Interfaces* 16, 30408–30420 (2024).
10. Ahmed, K. M., Muhammed, R. A., Omer, R. A., Azeez, Y. H. & Kareem, R. O. Design and Development of Innovative Thiourea-Based Compounds: Frontier Molecular Orbitals, Structural Optimization, Topological Characteristics, and Drug-Likeness Evaluations. *Chemistry Africa* 8, 1925–1935 (2025).
11. Abdelsalam, H. *et al.* Design and functionalization of halogenated hBN nanotubes for selective detection of halogenated volatile organic compounds: a DFT study. *Computational and Theoretical Chemistry* 1251, 115329 (2025).
12. Ahmed, M., Gupta, M. K. & Ansari, A. DFT and TDDFT exploration on the role of pyridyl ligands with copper toward bonding aspects and light harvesting. *J Mol Model* 29, 358 (2023).
13. Zhou, Z. *et al.* DFT calculation for organic semiconductor-based gas sensors: Sensing mechanism, dynamic response and sensing materials. *Chinese Chemical Letters* 36, 110906 (2025).
14. Mumit, M. A. *et al.* DFT studies on vibrational and electronic spectra, HOMO–LUMO, MEP, HOMA,

NBO and molecular docking analysis of benzyl-3-N-(2,4,5-trimethoxyphenylmethylene)hydrazinecarbodithioate. *Journal of Molecular Structure* 1220, 128715 (2020).

15. Wang, B., Sonar, P., Manzhos, S. & Haick, H. Diketopyrrolopyrrole copolymers based chemical sensors for the detection and discrimination of volatile organic compounds. *Sensors and Actuators B: Chemical* 251, 49–56 (2017).

16. Ullah, H., Shah, A.-H. A., Bilal, S. & Ayub, K. Doping and Dedoping Processes of Polypyrrole: DFT Study with Hybrid Functionals. *J. Phys. Chem. C* 118, 17819–17830 (2014).

17. Garg, S., Singla, R. & Goel, N. DFT Study on the Spin States of Polyaniline–3d Transition-Metal (Sc–Zn) Composites and Their Sensing Application to Detect Chemical Warfare Agents. *J. Phys. Chem. A* 128, 773–784 (2024).

18. Ingale, N., Tavhare, P. & Chaudhari, A. Hazardous molecules and VOCs sensing properties of Ti functionalized benzene: An ab initio study. *Sensors and Actuators A: Physical* 342, 113657 (2022).

19. Koparır, P. EXPERIMENTAL AND THEORETICAL ANALYSIS OF SOLVENTS EFFECT ON A DERİVATİVE OF CARBOTHIOAMIDE. *Journal of Physical Chemistry and Functional Materials* 7, 180–191 (2024).

20. Hu, W. & Chen, M. Editorial: Advances in Density Functional Theory and Beyond for Computational Chemistry. *Front. Chem.* 9, 705762 (2021).

21. Kaur, P., Bagchi, S., Pol, V. G. & Bhondekar, A. P. Early Detection of Mixed Volatile Organic Compounds to Circumvent Calamitous Li-Ion Battery Thermal Runaway. *J. Phys. Chem. C* 127, 8373–8382 (2023).

22. Jeanmairet, G., Levy, N., Levesque, M. & Borgis, D. Introduction to Classical Density Functional Theory by a Computational Experiment. *J. Chem. Educ.* 91, 2112–2115 (2014).

23. Kaur, P., Bagchi, S., Gribble, D., Pol, V. G. & Bhondekar, A. P. Impedimetric Chemosensing of Volatile Organic Compounds Released from Li-Ion Batteries. *ACS Sens.* 7, 674–683 (2022).

24. Anhaia-Machado, J. O. *et al.* Molecular Modeling Based on Time-Dependent Density Functional Theory (TD-DFT) Applied to the UV-Vis Spectra of Natural Compounds. *Chemistry* 5, 41–53 (2022).

25. Lee, S., Kim, M., Ahn, B. J. & Jang, Y. Odorant-responsive biological receptors and electronic noses for volatile organic compounds with aldehyde for human health and diseases: A perspective review.

Journal of Hazardous Materials 455, 131555 (2023).

26. Pratap Khare, K., Kathal, R., Shukla, N., Srivastava, R. & Srivastava, A. Orientation dependent DFT analysis of aniline and pyrrole based copolymer. *Materials Today: Proceedings* 47, 6934–6937 (2021).

27. Mardirossian, N. & Head-Gordon, M. Thirty years of density functional theory in computational chemistry: an overview and extensive assessment of 200 density functionals. *Molecular Physics* 115, 2315–2372 (2017).

28. Jayasundara, W. J. M. J. S. R. & Schreckenbach, G. Theoretical Study of p- and n-Doping of Polythiophene- and Polypyrrole-Based Conjugated Polymers. *J. Phys. Chem. C* 124, 17528–17537 (2020).

29. Raftani, M., Abram, T., Bennani, N. & Bouachrine, M. Theoretical study of new conjugated compounds with a low bandgap for bulk heterojunction solar cells: DFT and TD-DFT study. *Results in Chemistry* 2, 100040 (2020).

30. Nguyen, V. S. *et al.* Theoretical Study of Formamide Decomposition Pathways. *J. Phys. Chem. A* 115, 841–851 (2011).

31. Monari, A., Rivail, J.-L. & Assfeld, X. Theoretical Modeling of Large Molecular Systems. Advances in the Local Self Consistent Field Method for Mixed Quantum Mechanics/Molecular Mechanics Calculations. *Acc. Chem. Res.* 46, 596–603 (2013).

32. Cong, Y., Zhai, Y., Chen, X. & Li, H. The Accuracy of Semi-Empirical Quantum Chemistry Methods on Soot Formation Simulation. *IJMS* 23, 13371 (2022).

33. Andriianova, A. *et al.* Synthesis and Physico-chemical Properties of (Co)polymers of 2-[(2E)-1-methyl-2-buten-1-yl]aniline and Aniline. *Chin J Polym Sci* 37, 774–782 (2019).

34. Garg, S. & Goel, N. Tailoring Polypyrrole and Polyaniline Polymers by Introducing Side Groups for Sensing and Photovoltaic Applications: A DFT Study. *ACS Appl. Electron. Mater.* 4, 5246–5255 (2022).

35. Khanom, U., Saha, J. K., Jang, J. & Rahman, M. Revealing conducting organic polymers' interaction with cyanogen halides: DFT insights for enhanced gas sensing applications. *Struct Chem* 35, 1263–1272 (2024).

36. Lin, H. *et al.* Quantitation of volatile aldehydes using chemoselective response dyes combined with multivariable data analysis. *Food Chemistry* 353, 129485 (2021).

37. Chan, B. Optimal Small Basis Set and Geometric Counterpoise Correction for DFT Computations. *J. Chem. Theory Comput.* 19, 3958–3965 (2023).